Wavelength dependence of the preresonance Raman cross sections of CH_3CN, SO_4^{2-}, ClO_4^-, and NO_3^-

John M. Dudik, Craig R. Johnson, and Sanford A. Asher[a)]
Department of Chemistry, University of Pittsburgh, Pittsburgh, Pennsylvania 15260

(Received 5 October 1984; accepted 9 November 1984)

The Raman scattering cross sections of vibrations of SO_4^{-2}, NO_3^-, ClO_4^-, and CH_3CN have been determined between 220–640 nm. The cross sections of the symmetric stretching vibrations of SO_4^{-2} and ClO_4^- as well as the 918 cm^{-1} C–C stretching vibration of CH_3CN display almost a ν^4 excitation frequency dependence. The intensity of the 2249 cm^{-1} C≡N stretching vibration increases somewhat faster than ν^4, but significantly slower than that which would be expected if a dipole allowed C≡N $\pi \rightarrow \pi^*$ transition at ~150 nm dominated the Raman intensity. The intensity of the NO_3^- symmetric stretch increases with a frequency dependence close to that expected from an Albrecht *A* term contribution from the ~200 nm $\pi \rightarrow \pi^*$ transition. The fact that the 981 cm^{-1} SO_4^{-2}, 932 cm^{-1} ClO_4^-, and 918 cm^{-1} CH_3CN vibrations show essentially only ν^4 intensity dependencies indicates that no particular dipole allowed transition dominates the preresonance Raman intensities. These results suggest that conventional preresonance Raman expressions do not accurately model the Raman intensities. The small excitation frequency dependencies of SO_4^{-2}, ClO_4^-, and CH_3CN Raman intensities show that these species are ideal internal standards for Raman intensity measurements in the UV spectral region.

INTRODUCTION

The recent experimental and theoretical interest in resonance Raman spectroscopy stems from the potential utility of this technique as a probe of molecular structure in complex systems,[1-6] and as a technique for the assignment of electronic transitions,[7-9] and studies of vibronic interactions.[10] The large intensities observed with resonance excitation permits the selective study of individual species in complex samples. Resonance Raman spectroscopy has been extensively utilized to study chromophoric prosthetic groups in proteins such as hemes[11-13] and visual pigments.[14] Recently, extension of Raman spectroscopy into the UV spectral region has permitted studies of benzene derivatives,[15-18] polycyclic aromatic hydrocarbons,[19,20] aromatic amino acids and proteins,[21-23] and nucleic acids within cells.[24]

The experimental utility of Raman intensity measurements and experimental tests of resonance Raman theory require measurements of Raman excitation profiles. Because of difficulties inherent in measurements of absolute Raman intensities, Raman excitation profiles are generally measured relative to an internal intensity standard. Most previous excitation profile measurements in the visible and near UV spectral region utilized internal standards such as SO_4^{-2} [25] or cacodylate.[26] These species have their lowest energy absorption bands at wavelengths much shorter than that of the spectral region studied. It has been assumed with reasonable justification that these internal standard Raman intensities are essentially wavelength independent. Thus, the ratio of the analyte Raman intensity to that of the internal standard was used to directly monitor the Raman excitation profiles of the analyte.

As excitation occurs at shorter wavelengths it cannot be reasonably assumed that the internal standard Raman intensities are independent of wavelength. One approach has been to assume that internal standard intensities follow an Albrecht *A* term[27] intensity dependence with the resonant state assigned to the lowest energy $\pi \rightarrow \pi^*$ dipole allowed transition. This approach assumes that the lowest energy state dominates the preresonance Raman intensities. We show that this assumption is in general incorrect, and that it is necessary to directly measure the wavelength dependence of the Raman cross section of species which will be used as an internal intensity standard.

We have developed a new technique to measure the wavelength dependence of the relative Raman cross sections. By indexing these values to absolute Raman cross section data obtained by others in the visible spectral region we determine the wavelength dependence of the absolute Raman cross sections for compounds useful as internal Raman intensity standards. The dispersion of the Raman intensities gives new information on the vacuum UV electronic excited states of these molecules. Because of the spectral congestion in the vacuum UV few assignments of these electronic transitions exist.

EXPERIMENTAL

The Raman spectra were measured using a spectrometer described in detail elsewhere.[16] The excitation source is a Nd/Yag laser operated at 20 Hz with a

a) Corresponding author.

 0021-9606/85/041732-09$02.10

pulsewidth of 4 ns which was frequency doubled to pump a dye laser. UV radiation was generated by either frequency doubling the dye laser output or by mixing the doubled light with the 1.06 μm Yag fundamental. The scattered light was collected at 90° using reflective optics. The polarization of the scattered light was randomized by a crystalline quartz wedge polarization scrambler placed in front of the entrance slit of the monochromator. A Spex Triplemate monochromator dispersed the scattered light, and the dispersed light was detected by using an intensified Reticon detector.

The Raman scattered intensities were normalized to the laser intensity within the scattering volume by measuring both the Raman intensity and the intensity of elastic scattering of the laser light from a dispersion of $BaSO_4$ powder in the sample. The laser beam intensity was attenuated during measurements of the elastic scattering by using a series of calibrated, partially aluminized, suprasil neutral density filters obtained from Melles Griot [Irvine, California]. To avoid beam displacement or changes in beam focus in the sample upon introduction of the neutral density filters, identical unaluminized quartz plates replaced the neutral density filters during the Raman spectral measurements.

The samples used to directly measure the relative Raman cross sections of CH_3CN and SO_4^{-2} consisted of aqueous solutions of acetonitrile (3.8 M) and sodium sulfate (0.2 M). The UV spectral grade acetonitrile was obtained from Burdick and Jackson, and the sodium sulfate from Merck and Company. Ultra pure $BaSO_4$ powder, sold as a White Reflectance Standard,[28] was obtained from Eastman Kodak. This powder, which has a particle size of ~ 3 μm was added to the sample solution which was contained in a sealed standard 1 cm fluorescence cuvette. To keep the $BaSO_4$ powder suspended, the solution was stirred from the side during the spectral measurements with a small magnetic stirrer. Greater than 98% of the observed sulfate Raman intensity derived from dissolved sulfate in solution; the $BaSO_4$ powder contributed insignificantly to the SO_4^{2-} Raman intensity.

The barium sulfate powder packed as a dry pellet shows a diffuse reflectance which is almost independent of wavelength.[28] We experimentally demonstrated that the elastic scattering from a liquid dispersion of this powder changes only slowly with wavelength in the UV-visible spectral region. For example, Fig. 1 shows the apparent absorption spectrum of a dispersion of $BaSO_4$ in the sample solution. The attenuation of the beam results from light scattering by the $BaSO_4$ dispersion. We also determined that the intensity of 90° elastic light scattering from the $BaSO_4$ dispersion is also essentially independent of wavelength by using an Aminco–Bowman spectrofluorometer to measure 90° light scattering. The fluorometer throughput efficiency and the excitation beam intensity were determined by scattering the excitation beam from a packed powder of the $BaSO_4$ reflectance standard.

During the Raman measurements, the laser beam was directed into the cuvette with the beam focused above the cuvette to avoid dielectric breakdown and shock waves in the sample. The high peak power laser pulses, if focused within the sample, result in the breakup of the $BaSO_4$ particles, and an increased scattering occurs because of the increased number of particles. Absorption spectra of the sample solution were obtained before and after Raman excitation. No change in elastic scattering or sample absorption was observed between the spectral measurements.

The Raman and elastic scattered intensities were corrected for the spectrometer throughput efficiency. The Raman spectrometer throughput efficiency was calibrated in the UV by using a standard intensity deuterium lamp, and in the visible spectral region by using a standard intensity incandescent lamp. Light from the lamp was scattered from a Lambert surface prepared with the Kodak reflectance standard. A Polacoat UV polarizer was

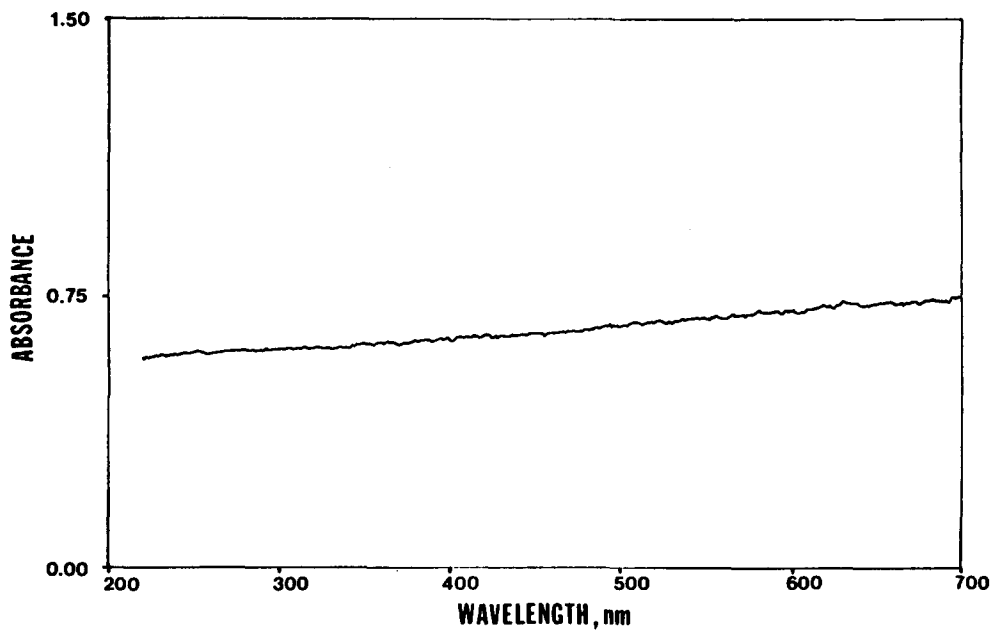

FIG. 1. The apparent absorption spectrum of the dispersion of $BaSO_4$ powder suspended in an aqueous solution of acetonitrile (3.8 M) and sulfate (0.2 M) used for the Raman cross section measurements.

used to measure the depolarization ratios in the UV. The laser intensity was measured before and after each Raman and elastic scattering measurement with a model 361 Scientech power meter. We typically observed less than a 3% standard deviation in the power level between measurements.

The relative Raman intensities were measured using both integrated areas and peak heights. The standard deviation of the peak height intensity ratios were smaller than those using peak areas, presumably because the peak height intensity ratios are less subject to random error due to incorrect subtraction of the background intensities. Thus, the relative intensity data plotted in Figs. 2–4 derive from the peak height measurements. Because the peak widths observed are dominated by the width of the spectrograph slit image on the detector the relative peak height ratios show only a weak dependence upon the spectrograph slitwidth and the frequency dispersion per Reticon detector pixel element. In addition, the band shapes of all of the Raman peaks studied, with the exception of the 2249 cm^{-1} CH_3CN peak, were essentially identical. We found essentially perfect agreement between the peak area and peak height ratio measurements for all but the 2249 cm^{-1} CH_3CN peak. The depolarization ratios were determined by using peak areas to avoid any systematic errors which could result from differences in the Raman band shapes between the polarized and depolarized spectra.

The wavelength dependence of the Raman cross sections of NO_3^- and ClO_4^- were determined relative to that of the 918 cm^{-1} peak of CH_3CN by comparing the intensities of the NO_3^- and ClO_4^- Raman peaks to that of the 918 cm^{-1} CH_3CN peak in aqueous solutions containing CH_3CN (3.8 M) and the ions (0.2 M).

THEORETICAL FRAMEWORK

The total vibrational Raman scattering cross section σ_{mn} for the vibrational transition $n \leftarrow m$ over 4π steradians for an isolated molecule averaged over all orientations is[29,30]

$$\sigma_{mn} = \frac{I_{mn}}{I_0} = \frac{2^7\pi^5}{3^2}\nu_0(\nu_0 - \nu_{mn})^3 g f(T)|\sum_{\rho\sigma}\alpha_{\rho\sigma}(\nu_0)|^2, \quad (1)$$

where I_{mn} is the integrated Raman scattered intensity (photons/s cm^2) over 4π steradians integrated over the bandwidth of the vibrational transition $n \leftarrow m$. I_0 and ν_0 are the incident excitation beam intensity and frequency (cm^{-1}), while ν_{mn} corresponds to the frequency of the Raman vibrational mode (cm^{-1}). g is a factor specifying the degeneracy of the initial state m while $f(T)$ is the Boltzmann weighting factor specifying the thermal occupancy of the initial state. The factor $\nu_0(\nu_0 - \nu_{mn})^3$ appears rather than $(\nu_0 - \nu_{mn})^4$ (as is commonly seen) because the intensities are defined in units of photons/s cm^2 for photon counting detection. $\alpha_{\rho\sigma}(\nu_0)$ is the ρ, σth (ρ, $\sigma = x$, y, z) component of the Raman polarizability tensor averaged over all molecular orientations for the excitation frequency, ν_0.

For 90° Raman scattering measurements from a solution where the incident light is polarized perpendicular to the scattering plane, and both the parallel and perpendicular scattering polarization are collected, the differential Raman scattering cross section, σ_R is given by[29,30]

$$\sigma_R = \frac{d\sigma_{mn}(\nu_0)}{d\Omega} = \frac{2^4\pi^4}{45} b^2 g \frac{L\nu_0(\nu_0 - \nu_{mn})^3}{1 - \exp(-hc\nu_{mn}/kT)}(45\alpha^2 + 7\gamma^2), \quad (2)$$

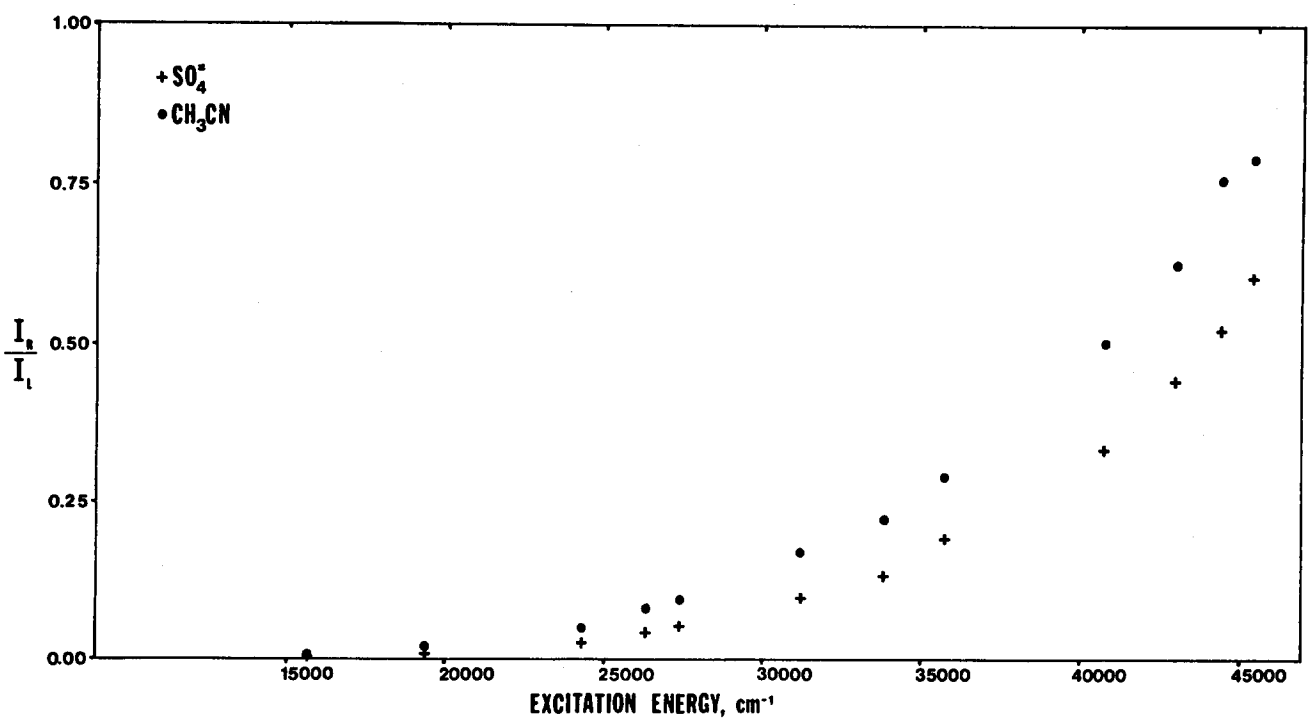

FIG. 2. The excitation frequency dependence of the relative Raman intensities of acetonitrile's 918 cm^{-1} C–C stretch and sulfate's 981 cm^{-1} stretch referenced to the intensity of the elastically scattered laser line through the UV-visible spectral regions.

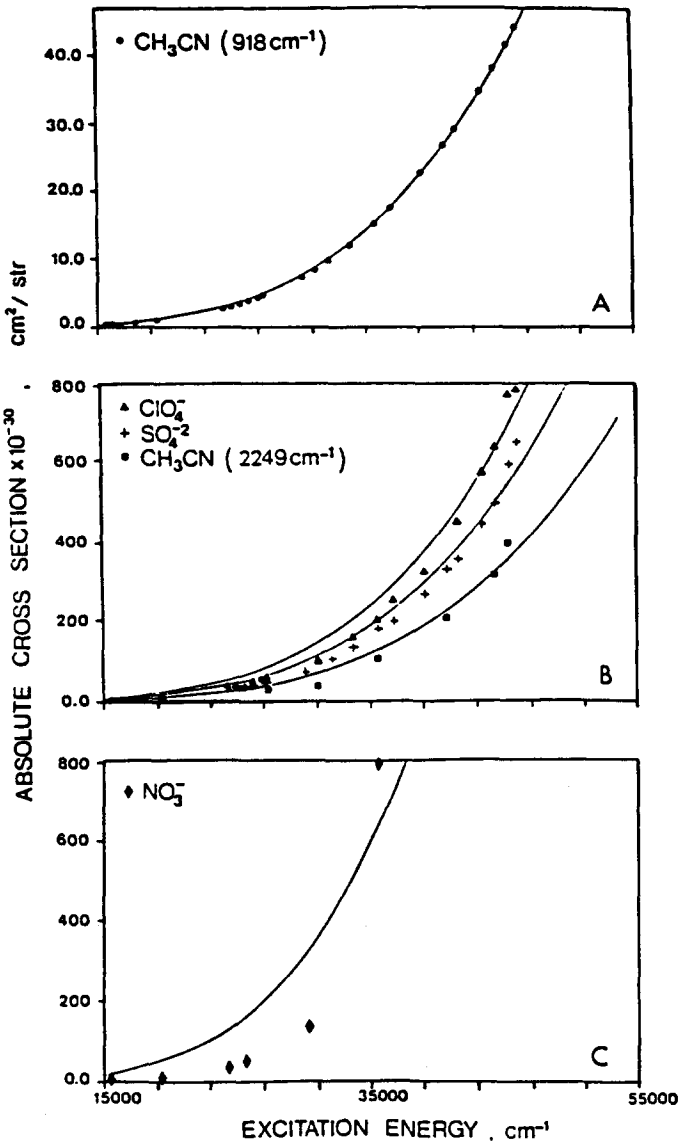

FIG. 3. Absolute Raman cross sections of (A) the 918 cm^{-1} C–C stretch of acetonitrile. (B) The 2249 cm^{-1} C ≡ N stretch of acetonitrile, the 932 cm^{-1} stretch of perchlorate, the 981 cm^{-1} stretch of sulfate. (C) The 1045 cm^{-1} stretch of nitrate. The solid curves represent the best fit of the data to the $\nu_0(\nu - \nu_{mn})^3$ frequency dependence. See the text for details.

where b is the zero point vibrational amplitude:

$$b = (h/8\pi c^2 \nu_{mn})^{1/2}$$

and α^2 and γ^2 are the isotropic and anisotropic invarients of the polarizability tensor, respectively. h, c, k, T are Planck's constant, the speed of light, Boltzmann's constant, and the temperature, respectively. L is the local field correction for the condensed phase sample which specifies the increased electric field amplitude in the sample over that which would be present in the gas phase. L is suggested to be[29,32]

$$L = (n_s/n_0)(n_s^2 + 2)^2(n_0^2 + 2)^2/81, \quad (3)$$

where n_s and n_0 are the sample refractive indices at $(\nu_0 - \nu_{mn})$ and ν_0.

The experimentally observed intensity of the Raman scattered light depends upon the collection optics and the transfer function of the Raman spectrometer. Thus, the observed Raman intensity can be expressed as

$$I_{mn} = N_M I_0 F(\theta) S(\nu_R) E(\nu_R) \sigma_R(\nu_0). \quad (4)$$

N_M is the number of molecules contained in the scattering volume. $F(\theta)$ represents the fraction of the scattered light imaged into the spectrometer. $S(\nu_R)$ is the transmittance of the Raman scattered light out of the sample; attenuation occurs due to $BaSO_4$ particle scattering. $E(\nu_R)$ is the throughput efficiency of the spectrometer for the Raman scattered frequency, and $\sigma_R(\nu_0)$ is the Raman scattering cross section for an excitation frequency of ν_0.

The advantage of our method over previous cross section measurement techniques[33–35] is that the collection geometry remains the same for both the Raman and elastic scattering measurements, and the elastic scattering intensity directly monitors the incident laser intensity in the illuminated sample volume. The observed elastically scattered intensity, I_L can be expressed as

$$I_L = N_B I_0 T(\nu_0) F(\theta) S(\nu_0) E(\nu_0) \sigma_B(\nu_0), \quad (5)$$

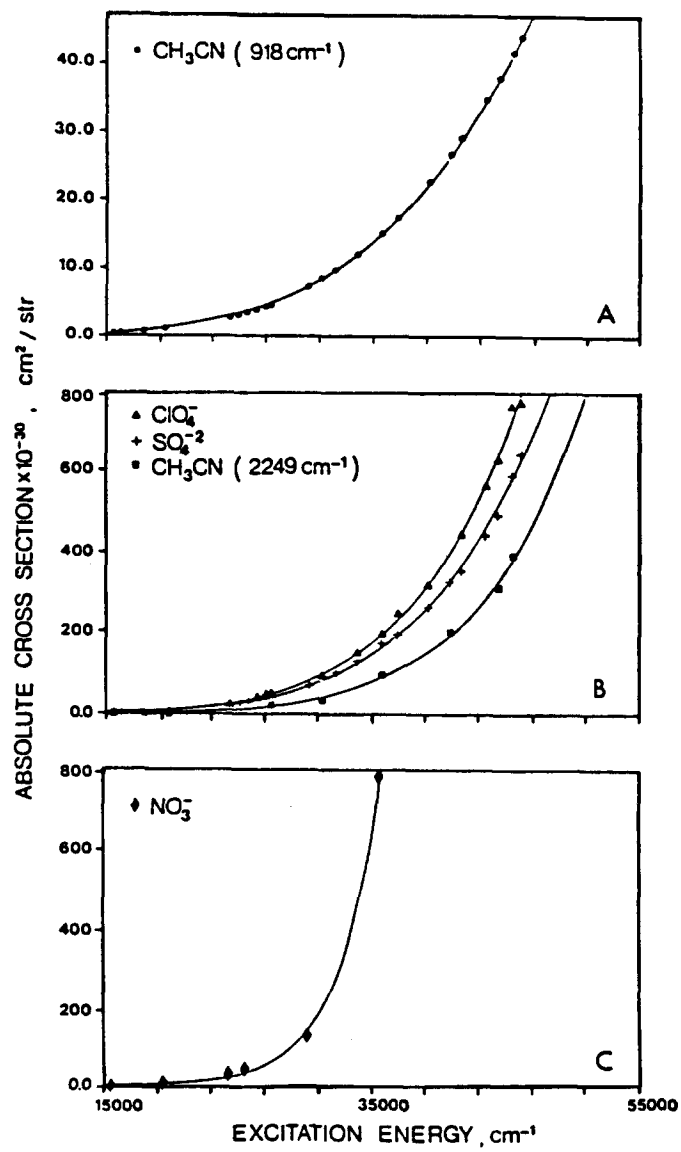

FIG. 4. The absolute Raman cross section data from Fig. 3 fitted to Albrecht's A term [Eq. (11)].

where N_B is the number of barium sulfate particles in the scattering volume, $T(\nu_0)$ is the transmittance of the neutral density filters, $S(\nu_0)$ is the transmittance of the elastically scattered light out of the sample, and $E(\nu_0)$ is the efficiency throughput of the spectrometer for the excitation frequency ν_0. $\sigma_B(\nu_0)$ is the $BaSO_4$ scattering cross section per particle. Because the sampling geometry is identical for both the Raman and elastic scattering measurement, and $S(\nu_0) \cong S(\nu_0 - \nu_{mn})$ as can be seen from Fig. 1, the Raman scattering cross section can be written:

$$\sigma_R(\nu_0) = T(\nu_0)\frac{N_B}{N_M}\frac{I_{mn}}{I_L}\frac{E(\nu_0)}{E(\nu_R)}\sigma_B(\nu_0). \quad (6)$$

The wavelength dependence of the differential elastic scattering cross section of a barium sulfate particle, $\sigma_B(\nu_0)$ can be determined from a transmission measurement of the sample solution. The attenuation $dP(\nu_0)$ of an incident beam of intensity $P_0(\nu_0)$ per unit length in the sample solution is given by

$$dP(\nu_0) = -\rho_B\sigma_B(\nu_0)P_0(\nu_0)dx,$$

where ρ_B is the barium sulfate particle number density and dx is the length traveled by the incident beam. Thus,

$$-\log P(\nu_0)/P_0(\nu_0) = \frac{\rho_B\sigma_B(\nu_0)X}{2.303} = A(\nu_0),$$

so

$$\sigma_B(\nu_0) = \frac{2.303\,A(\nu_0)}{\rho_B X}, \quad (7)$$

where $A(\nu_0)/X$ is the apparent absorbance of the sample per unit pathlength due to scattering from $BaSO_4$ particles. Therefore,

$$\sigma_R(\nu_0) = \frac{2.303\,T(\nu_0)N_BI_{mn}E(\nu_0)}{N_MI_LE(\nu_R)}\frac{A(\nu_0)}{\rho_BX}. \quad (8)$$

The excitation frequency dependence of the differential Raman scattering cross section can be easily calculated from Eq. (8) since the transmittance of the neutral density filters and the throughput efficiency of the monochromator are known, and the absorbance of the sample due to $BaSO_4$ scattering is easily measured (see Fig. 1). The absolute value of the cross section could be obtained if the ratio N_B/N_M and ρ_B were known; however, it is easier to obtain the cross section by indexing the relative Raman cross section to previously determined cross sections obtained by others by using excitation with cw lasers in the visible spectral region.

RESULTS

Figure 2 shows the excitation frequency dependence of σ_R observed for the 981 cm^{-1} sulfate symmetric stretch and the 918 cm^{-1} acetonitrile C–C stretching vibration. The data plotted in Fig. 2 are directly proportional (within the factor $N_B2.303/N_M\rho_B$) to the Raman scattering cross sections since the observed I_{mn}/I_0 ratios have been corrected for the neutral density filter transmittances, the spectrometer throughput efficiencies and the apparent sample absorbance as prescribed by Eq. (8). As expected, the Raman cross sections increase as the excitation frequency increases. The cross section of the sulfate 981 cm^{-1} vibration increases somewhat faster than that of the 918 cm^{-1} acetonitrile vibration.

The absolute differential Raman scattering cross section of the data shown in Fig. 2 can be determined by indexing the relative differential cross section data to a measured absolute Raman cross section. Thus, we prepared a benzene solution (1.2 M) in acetonitrile and measured the intensity of the 992 cm^{-1} benzene symmetric stretch relative to the 918 cm^{-1} CH_3CN vibration. The absolute Raman scattering cross section of the 918 cm^{-1} vibration of acetonitrile is obtained from

$$(\sigma_R)_{918} = (\sigma_R)_{992}\left(\frac{I_{918}}{I_{992}}\right)\left[\frac{E(\nu_0 - 992)}{E(\nu_0 - 918)}\right]\left(\frac{C_B}{C_A}\right)L, \quad (9)$$

where C_A and C_B are the concentrations of acetonitrile and benzene, respectively. We used the 514.5 nm value of the differential Raman scattering cross section of liquid benzene of Abe *et al.*[32] 28.6×10^{-30} cm^2/molecule sr and used the local field correction of Eq. (3) to obtain a cross section of 19.2×10^{-30} cm^2/molecule sr for benzene dissolved in CH_3CN. We assume the refractive index of the solution is a volume weighted average of the contribution of the benzene and CH_3CN. Thus the refractive index of the solution is 1.36.

We used the resulting absolute total Raman cross section value of $(\sigma_R)_{918} = 1 \times 10^{-30}$ cm^2/molecule sr at 514.5 nm excitation to determine the Raman cross sections of other species. Figure 3 shows the excitation frequency dependence of the absolute total differential cross sections of the 918 cm^{-1} CH_3CN vibration, and the 981 cm^{-1} SO_4^{-2}, the 932 cm^{-1} ClO_4^-, the 1045 cm^{-1} NO_3^- symmetric stretching vibrations, as well as the 2249 cm^{-1} C≡N stretch of CH_3CN. These data were obtained by measuring the intensities of these species relative to the 918 cm^{-1} CH_3CN vibration and by using Eq. (9).

We also measured the depolarization ratios, ρ for these vibrations. Due to the finite solid angle of the collection optics, and the residual transmittance of the UV polarization analyzer for the perpendicular polarization we can only determine an upper limit for the UV depolarization ratios. Within this upper limit we observe no change ($\Delta\rho \leq \pm 0.03$) in the depolarization ratios of the 981 cm^{-1} peak of SO_4^{-2} or the 918 cm^{-1} peak of acetonitrile with excitation between 640 and 220 nm. The most likely value for ρ for all of these species is less than $\rho = 0.05$ for excitation between 300–220 nm. For the remaining discussion we assume that no dispersion exists in the depolarization ratio between 640–220 nm for any of the species studied. Table I lists the Raman cross sections for these species at 514.5, 280.0, and 220.0 nm.

The frequency dependence of our Raman cross section data compare favorably with the few prior studies which examined the excitation frequency dependence of the Raman cross section. Hoffman and Moser[36] compared the Raman scattering cross sections of SO_4^{2-} excited by the mercury lines at 253.7 and 435.8 nm. They obtained

TABLE I. Measured total differential Raman cross sections using peak heights and peak areas. Also included are the parameters for the Albrecht A term fits shown in Fig. 4. We expect the likely error in the cross section measurements is less than 20%.

$$\sigma_R = K_2\nu_0(\nu_0 - \nu_{mn})^3\left[\frac{\nu_e^2 + \nu_0^2}{(\nu_e^2 - \nu_0^2)^2}\right]^2.$$

	Absolute Raman cross section × 10^{-30} cm^2/molecule sr			A-term fit		
Molecule/Band	514.5 nm	280.0 nm	220.0 nm	K_2 (cm^2/molecule sr)	ν_e (cm^{-1})	λ_e (nm)
CH_3CN/918 cm^{-1}	1.00[a] 1.01[b]	15.2	41.6	2.26×10^{-25}	390 000	25.7
CH_3CN/2249 cm^{-1}	5.62[a] 8.22[b]	103	399	7.65×10^{-27}	116 000	86.2
ClO_4^-/932 cm^{-1}	10.4[a] 12.7[b]	204	772	2.34×10^{-26}	128 000	78.1
SO_4^{-2}/981 cm^{-1}	9.92[a] 9.90[b]	183	601	2.75×10^{-26}	137 000	72.9
NO_3^-/1045 cm^{-1}	10.1[a] 10.9[b]	799	...	1.56×10^{-28}	52 300	191

[a] Peak height.
[b] Peak area.

a ratio of 18 for the Raman cross sections. The data shown in Fig. 4 agree well and give a ratio of 16.8. Using the Raman cross sections of the 918 cm^{-1} CH_3CN peak we experimentally determined the ratio of the cross sections of benzene at 337.1 and 514.5 nm and obtained a ratio of 10.6. Abe *et al.*[32] using identical wavelengths found ratios of 13.6 for benzene dissolved in cyclohexane and 10.6 for benzene in the gas phase. Abe *et al.* relative ratios of the liquid phase benzene cross sections derive from: (1) Measurements of the Raman cross section of cyclohexane in the gas phase obtained by using the intensity of the H_2 rotational Raman lines as a reference. (2) The liquid phase cross section of cyclohexane was determined by using a local field correction. (3) The relative Raman intensity of benzene compared to cyclohexane resulted in the liquid phase benzene Raman cross sections. It is likely that our results are somewhat more accurate than those of Abe *et al.*,[32] in view of the poor signal to noise ratio they suggested for their 337 nm data.

Our Raman cross section for SO_4^{-2} of 29×10^{-30} cm^2 sr^{-1} molecule^{-1} at 413 nm is close to the recent cross section measurement of an aqueous solution of $(NH_4)_2SO_4$ by Stallard *et al.*[37] who obtained a value for the polarized differential cross section, σ_{RP} of 32×10^{-30} cm^2 sr^{-1} molecule^{-1}; since the depolarization ratio is 0.03, the total differential cross section would be $\sigma_R = (1 + \rho)\sigma_{RP} = 33 \times 10^{-30}$ cm^2 sr^{-1} molecule^{-1}. Our cross section value for SO_4^{-2} with 514.5 nm excitation of 9.9×10^{-30} cm^2 sr^{-1} molecule^{-1} is also close to the total differential cross section measured by Myers *et al.*[38] of 11.0×10^{-30} cm^2 sr^{-1} molecule^{-1}.

DISCUSSION

The excitation frequency dependence of the Raman scattering cross section is given by

$$\sigma_R(\nu_0) = KL(\nu_0)\nu_0(\nu_0 - \nu_{mn})^3[\alpha(\nu_0)]^2, \quad (10)$$

where K is a constant which can be evaluated from Eq. 2. $L(\nu_0)$ is the correction factor for the local electric field and depends upon the refractive indices at the excitation and Raman scattered frequencies [Eq. (3)]. We determine the Raman cross section through a relative measurement using an internal standard in a nonabsorbing solution, and the difference in the refractive index is small over the $\sim$100 cm^{-1} Raman frequency difference between the two vibrations; as a result, the contribution of $L(\nu_0)$ to the frequency dependence of σ_R is negligible. Thus, the frequency dependence of σ_R derives from the $\nu_0(\nu_0 - \nu_{mn})^3$ factor and any dispersion or preresonance enhancement shown by the invarients of the polarizability tensor $[\alpha(\nu_0)]^2$.

The solid lines in Fig. 3 show a least squares best fit of the data to a $\nu_0(\nu_0 - \nu_{mn})^3$ frequency dependence. Figure 3(a) shows that the intensity of the 918 cm^{-1} CH_3CN peak varies almost exactly as $\nu_0(\nu_0 - \nu_{mn})^3$ and indicates that only a minor preresonance enhancement occurs for this peak. $\nu_0(\nu_0 - \nu_{mn})^3$ fits to the excitation profiles of the 932 cm^{-1} ClO_4, 981 cm^{-1} SO_4^{-2}, and the 2249 cm^{-1} CH_3CN vibrations are somewhat less satisfactory; the high and low frequency data show deviations above and below the fitted curve, respectively. This indicates that a small but significant preresonance enhancement occurs for these species. The fit for the 1045 cm^{-1} NO_3^- data is clearly unacceptable and indicates that preresonance enhancement dominates the frequency dependence of the Raman cross sections.

Each of the vibrational modes derives from symmetric stretching vibrations. If the preresonance enhancement were dominated by one electronic transition at higher energy the preresonance frequency dependence of the polarizability tensor invarients could be approximated by

an Albrecht A term expression which gives the following relationship for the excitation frequency dependence of the Raman cross sections:

$$\sigma_R(\nu_0) = K_2\nu_0(\nu_0 - \nu_{mn})^3\left[\frac{\nu_e^2 + \nu_0^2}{(\nu_e^2 - \nu_0^2)^2}\right]^2, \quad (11)$$

where K_2 is a constant, and ν_e is the frequency of the transition to the resonant excited state.

All of the cross section data in Fig. 3 were fitted to Eq. (11) by a nonlinear least squares analysis. The results of the fit are shown as solid lines in Fig. 4 and the resulting transition energies are listed in Table I. The fit of the 918 cm^{-1} CH_3CN data to Eq. (11) results in only a slight improvement over the $\nu_0(\nu_0 - \nu_{nm})^3$ fit shown in Fig. 3(a). The electronic transition is calculated to occur far in the UV at 389 000 cm^{-1} (25.7 nm). This was expected from the fit shown in Fig. 3(a); little dispersion of the Raman polarizability tensor is evident. Similarly, the transition energies calculated for the ClO_4^-, SO_4^{-2}, and the 2249 cm^{-1} CH_3CN vibrations also occur in the far UV at ~128 000 cm^{-1} (78.1 nm), 137 000 cm^{-1} (72.9 nm), and 116 000 cm^{-1} (86.2 nm). The only peak showing a resonant state in the low energy UV is the 1045 cm^{-1} NO_3^- vibration which shows a transition at 52 300 cm^{-1} (191 nm). Also shown in Table I are the K_2 values of Eq. (11).

The A term fits using Eq. (11) result in cross section frequency dependences in excellent agreement with the data. However, the approximations involved in Eq. (11) probably lead to overestimates of the transition energies of the lowest energy excited states important for the preresonance enhancement of these vibrations. The A term fit assumes that one transition dominates the Raman intensities. Actually numerous transitions must contribute to the polarizability tensor. These contributions could be of opposite sign and lead to partial cancellation of the contribution of pairs of transitions. It is likely that a simple A term fit will result in an overestimate of the transition energy for the closest lying state contributing to the Raman intensity.

For the 918 cm^{-1} CH_3CN C–C stretching vibration essentially no preresonance enhancement is evident. Vacuum UV absorption spectra of CH_3CN show an onset of absorption at 180 nm with strong broad absorption features below 170 nm.[39–43] These observed transitions could involve $\pi \rightarrow \pi^*$, $n \rightarrow \pi^*$, Rydberg, and $\sigma \rightarrow \pi^*$ transitions, as well as, charge transfer transitions between the solvent and the sample molecules. The ionization limit from the highest occupied molecular orbitals should occur at wavelengths longer than 100 nm (98 600 cm^{-1} for CH_3CN).[42]

The C–C stretching vibration is unlikely to be strongly enhanced by the C≡N $\pi \rightarrow \pi^*$ and $n \rightarrow \pi^*$ transitions, or by Rydberg transitions where π electrons are promoted to large diffuse atomic like orbitals.[44] However, $\sigma \rightarrow \sigma^*$ or $\sigma \rightarrow \pi^*$ transitions might give strong enhancement. To the extent that allowed $\sigma \rightarrow \sigma^*$ or $\sigma \rightarrow \pi^*$ transitions exist in the poorly understood vacuum UV spectra, they are expected to occur at wavelengths in the range of 100 nm.[39–44] We tentatively conclude that the lack of preresonance enhancement for the 918 cm^{-1} CH_3CN stretch occurs because no suitable electronic transition exists below 100 000 cm^{-1} (100 nm) to dominate the Raman intensity.

A larger preresonance enhancement is evident for the 2249 cm^{-1} peak of CH_3CN. The resonant state as fitted by an A term expression occurs at 116 000 cm^{-1} (86.2 nm). The decreased excited state frequency results from a strong contribution to the Raman intensity of transitions at energies below 150 000 cm^{-1}. An allowed $\pi \rightarrow \pi^*$ transition in CH_3CN has not been assigned, but it is expected to be important in the preresonant enhancement of the C≡N stretching vibration. The Rydberg transition at 73 500 cm^{-1} (~130 nm) from the highest occupied C≡N orbital to a 3s Rydberg orbital shows vibronic structure from the 2249 cm^{-1} C≡N stretching vibration.[41–43] This transition may contribute to the preresonance Raman intensity.

The A term fits for the symmetric stretching vibrations of ClO_4^- and SO_4^{-2} result in transition energies of 128 000 cm^{-1} (78.1 nm) and 137 000 (72.8 nm), respectively. Thus, as for CH_3CN no low energy transitions appear to dominate the Raman intensities. Although strong UV absorption is evident for these species at energies above 50 000 cm^{-1} (200 nm), these absorption bands are assigned as charge transfers between the ion and the aqueous solution.[43,45–47] It is not obvious that these transitions should lead to strong enhancement of the symmetric stretching vibrations of these ions. Assignments for the $\pi \rightarrow \pi^*$ transition energies for these species are not available.

Nitrate shows a weak absorption band at 300 nm ($\epsilon \sim 7$) assigned to an $n \rightarrow \pi^*$ transition and a strong absorption band at 200 nm ($\epsilon \sim 10\,000$) assigned to a $\pi \rightarrow \pi^*$ transition.[43,48,49] The low molar absorptivity of the 300 nm band is unlikely to result in any significant resonance enhancement, and no obvious contribution from it is evident in the NO_3^- excitation profile; no resonance enhancement is observed in the 274 nm $n \rightarrow \pi^*$ transition of acetone.[50] The A term fit to the NO_3^- excitation profile results in a transition energy of 52 300 cm^{-1} (191 nm), close to the position of the $\pi \rightarrow \pi^*$ absorption spectral maximum. Thus, the data indicate that the presence of an isolated low energy allowed transition does result in a preresonance enhancement which is well modeled by the A term. For NO_3^- essentially *all* of the Raman intensity between 640–220 nm derives from the 200 nm absorption band.

As discussed previously the simple A term fit is likely to overestimate the energy of the lowest energy preresonance transition. Another approach to estimating the energy of the lowest transition contributing to the Raman intensity would be to modify the Albrecht A term expression to include contributions from additional states. For all of the species studied, including benzene,[15] the excitation profile far from resonance increases more slowly than would be expected from one electronic transition. As resonance is approached the lowest energy electronic transition begins to dominate the preresonance enhance-

TABLE II. Estimated transition energies derived from nonlinear least squares fits to Eqs. (11) and (12).

	ν_e Eq. (11)		ν_e Eq. (12)	
Vibrational mode	cm^{-1}	nm	cm^{-1}	nm
$CH_3CN/918\ cm^{-1}$	390 000	25.7	142 000	70
$CH_3CN/2249\ cm^{-1}$	116 000	86.2	62 000	162
$ClO_4^-/932\ cm^{-1}$	128 000	78.1	75 000	133
$SO_4^{-2}/981\ cm^{-1}$	137 000	72.9	71 000	140
$NO_3^-/1045\ cm^{-1}$	52 300	191	42 500	235

ment and the observed intensity increase is modeled well by Eq. (11). The preresonant enhancement can then be phenomenologically modeled by adding the contribution of a state at very high energy which gives rise to a frequency independent contribution to the intensity

$$\sigma_R(\nu_0) = K_3\nu_0(\nu_0 - \nu_{mn})^3\left[\frac{\nu_e^2 + \nu_0^2}{(\nu_e^2 - \nu_0^2)^2} + K_4\right]^2. \quad (12)$$

This expression should lead to underestimates of the energy of the resonant transition important for preresonance enhancement. Table II compares the transition energies obtained using Eqs. (11) and (12). As expected, the transition energies decrease dramatically, and for NO_3^- the transition energy is underestimated by the fit using Eq. (12). The fits using Eq. (12) are only slightly better than those using Eq. (11). The energies of the important preresonant electronic transition should be bracketed by the transition energies calculated using Eqs. (11) and (12).

The results clearly indicate that the important electronic transitions giving Raman intensity to the C≡N stretching vibration of CH_3CN occur at lower energies than those transitions contributing intensity to the C–C stretch. Indeed, the $\pi \rightarrow \pi^*$ transition in CH_3CN should occur at an energy close to 62 000 cm^{-1}. ClO_4^- should have its $\pi \rightarrow \pi^*$ or intramolecular charge transfer transitions at somewhat lower energy than that of SO_4^{-2}.

CONCLUSIONS

With the recent advances in Raman instrumentation it is now possible to measure excitation profiles of "small" polyatomic molecules in the UV. This report characterizes the excitation frequency dependence of the Raman intensities for a series of molecules and ions which can serve as internal standards. All of these, except for NO_3^-, have vibrational modes whose intensities almost follow a $\nu_0(\nu_0 - \nu_{mn})^3$ dependence. The transition energies given in Tables I and II allow workers to determine the excitation frequency dependence of the Raman intensities of these species by using the A term expression, and the constants given in Table I. Thus, these species can be used as internal standards to determine absolute Raman excitation profiles and absolute Raman cross sections in the visible through the UV spectral region down to 220 nm.

The preresonance excitation profiles probe the excited states in the poorly understood vacuum UV. To the extent that valence transitions ($\pi \rightarrow \pi^*$, $\sigma \rightarrow \pi^*$, etc.) exist at this energy they should contribute to the Raman intensity. However, most of these transitions occur at the same energies as Rydberg and ionizing transitions. Thus, there may be no discrete transitions in the far UV (especially in the condensed phase). Raman excitation in the far UV will be required to properly interpret the preresonance Raman results obtained here.

ACKNOWLEDGMENTS

We gratefully acknowledge Thanh Phung for technical help in these studies and Edward Zipf for the use of his standard intensity lamps and for helpful discussions. We also gratefully acknowledge support for this study from NSF instrumentation grant PCM-8115738 and NIH grant No. 1R01 GM 30741-03. Acknowledgment is also made to the Donors of the Petroleum Research Fund administered by the American Chemical Society for starter grant PRF #13264G46. S. A. Asher is an Established Investigator of the American Heart Association.

[1] P. R. Carey, *Biochemical Applications of Raman and Resonance Raman Spectroscopy* (Academic, New York, 1982).
[2] A. T. Tu, *Raman Spectroscopy in Biology: Principles and Applications* (Wiley, New York, 1982).
[3] D. A. Long, *Raman Spectroscopy* (McGraw-Hill, New York, 1977).
[4] S. A. Asher and C. R. Johnson, Science **225,** 311 (1984).
[5] G. J. Thomas and L. A. Day, Proc. Natl. Acad. Sci. U.S.A. **78,** 2962 (1981).
[6] C. R. Johnson and S. A. Asher, Anal. Chem. **56,** 2258 (1984).
[7] R. J. H. Clark and B. Stewart, Struct. Bonding (Berlin) **36,** 1 (1979).
[8] S. A. Asher and K. Sauer, J. Chem. Phys. **64,** 4115 (1976).
[9] A. Y. Hirakawa and M. Tsuboi, *Vibrational Spectra and Structure,* edited by J. R. Durig (Elsevier, New York, 1983), p. 145.
[10] W. Siebrand and M. Z. Zgierski, *Excited States IV* (Academic, New York, 1979), p. 1.
[11] S. A. Asher, Methods in Enzymol. **76,** 371 (1981).
[12] D. L. Rousseau, J. M. Friedman, and P. T. Williams, *Topics in Current Physics* (Springer, Berlin, 1979), Vol. 11, p. 203.
[13] T. G. Spiro, in *Iron Porphyrins,* edited by A. B. P. Lever and H. B. Gray (Addison-Wesley, Reading, Mass, 1983), pt. II, p. 89.
[14] R. Mathies, *Chemical and Biochemical Applications of Lasers,* edited by C. B. Moore (Academic, New York, 1979), p. 55.
[15] S. A. Asher and C. R. Johnson, J. Phys. Chem. (in press).
[16] S. A. Asher, C. R. Johnson, and J. Murtaugh, Rev. Sci. Instrum. **54,** 1657 (1983).
[17] L. D. Zeigler and B. S. Hudson, J. Chem. Phys. **79,** 1134 (1983).
[18] L. D. Zeigler and B. S. Hudson, J. Chem. Phys. **74,** 982 (1981).
[19] S. A. Asher, Anal. Chem. **56,** 720 (1984).
[20] W. L. Peticolas, L. Chinsky, P-Y. Turpin, and A. Laigle, J. Chem. Phys. **78,** 656 (1983).
[21] R. P. Rava and T. G. Spiro, J. Am. Chem. Soc. **106,** 4062 (1984).
[22] M. H. Baron, C. deLoze, T. Mejean, M. J. Coulange, P. Y. Turpin, and L. Chinsky, J. Chem. Phys. (Paris) **80,** 730 (1983).
[23] C. R. Johnson, M. Ludwig, S. E. O'Donnell, and S. A. Asher, J. Am. Chem. Soc. **106,** 5008 (1984).
[24] L. Chinsky, P. Y. Turpin, M. Duquesne, and J. Brahms, Biopolymers **17,** 1347 (1978).
[25] M. Tsuboi, A. Y. Hirakawa, Y. Nishimura, T. Matsumoto, and M. Nakanishi, J. Raman Spectrosc. **7,** 282 (1978).
[26] D. C. Blazej and W. L. Peticolas, Proc. Natl. Acad. Sci. U.S.A. **74,** 2639 (1980); J. Chem. Phys. **72,** 3134 (1980).
[27] A. C. Albrecht and M. C. Hutley, J. Chem. Phys. **55,** 4438 (1971).
[28] F. Grum and G. W. Luckey, Appl. Opt. **7,** 2289 (1968).
[29] H. W. Schrotter and H. W. Klochner, *Topics in Current Physics,* edited by A. Weber (Springer, Berlin, 1979), p. 123.

[30] G. Eckhardt and W. G. Wagner, J. Mol. Spectrosc. **19,** 407 (1966).
[31] M. J. Colles and J. Griffiths, J. Chem. Phys. **56,** 3384 (1972).
[32] N. Abe, M. Wakayama, and M. Ito, J. Raman Spectrosc. **6,** 38 (1977).
[33] Y. Kato and T. Hiroshi, J. Chem. Phys. **54,** 5398 (1971).
[34] Y. Kato and H. Tokumo, J. Opt. Soc. Am. **61,** 347 (1971).
[35] W. G. Nilsen and J. G. Skinner, J. Opt. Soc. Am. **58,** 113 (1968).
[36] W. Hofmann and H. Moser, Ber. Bunsenges. Phys. Chemie **68,** 129 (1964).
[37] B. R. Stallard, P. R. Callis, P. M. Champion, and A. C. Albrecht, J. Chem. Phys. **80,** 70 (1984).
[38] A. B. Myers, R. B. Harris, and R. A. Mathies, J. Chem. Phys. **79,** 603 (1983).
[39] G. Herzberg and G. Scheibe, Z. Phys. Chem. Abt. B **7,** 390 (1930).
[40] J. A. Cutler, J. Chem. Phys. **16,** 136 (1948).
[41] M. N. R. Ashfold and J. P. Simons, J. Chem. Soc. Faraday Trans. 2 **74,** 1263 (1978).
[42] R. F. Lake and H. Thompson, Proc. R. Soc. London Ser. A **317,** 187 (1970).
[43] M. B. Robin, *Higher Excited States of Polyatomic Molecules* (Academic, New York, 1975), Vol. II.
[44] M. B. Robin, *Higher Excited States of Polyatomic Molecules* (Academic, New York, 1974), Vol. I.
[45] E. Rabinowitch, Rev. Mod. Phys. **14,** 112 (1942).
[46] J. L. Weeks, G. M. A. C. Meaburn, and S. Gordon, Radiat. Res. **19,** 559 (1963).
[47] L. E. Orgel, Q. Rev. (London) **8,** 422 (1954).
[48] J. A. Friend and L. E. Lyons, J. Chem. Soc. **1959,** 1572.
[49] K. L. McEwen, J. Chem. Phys. **34,** 547 (1961).
[50] J. M. Dudik, C. R. Johnson, and S. A. Asher, J. Phys. Chem. (in preparation).